Transport Physics of Hybrid Scenario Plasmas in the International Multi-Tokamak Database and Implications for ITER [1]

R.V.Budny 1), C.E.Kessel 1), J.E.Kinsey 2), F.Imbeaux 3), I.Voitsekhovitch 4), J.Candy 5), R.E.Waltz 5), T.Fujita 6), C.M.Greenfield 5), M.Murakami 7), A.C.C.Sips 8), W.A.Houlberg 7), E.J.Doyle 9), for the ITPA Topical Group on Transport Physics and the ITPA Profile Database Working Group

1) Princeton Plasma Physics Laboratory, P.O. Box 451, Princeton, NJ 08543-0451, USA
2) Lehigh University, Bethlehem, PA 18015, USA
3) Association EURATOM-CEA, Cadarache F-13108 Saint-Paul-lez-Durance Cedex,FR
4) EURATOM/ UKAEA Fusion Association, Abingdon, OX14 3DB, United Kingdom
5) General Atomics, PO Box 85608, San Diego, CA 92186, USA
6) Naka Fusion Research Establishment, JAEA, Nakamachi, Naka-gun, Ibaraki-ken, JP
7) Oak Ridge National Laboratory, Oak Ridge, TN, USA
8) Max-Planck-Institute fur Plasmahysik, EURATOM-IPP Association, Garching, GDR
9) University of California, Los Angeles, CA 90095-1365, USA

e-mail contact of main author: budny@princeton.edu

Abstract. Transport in Hybrid plasmas in the international ITPA profile database is studied. The TRANSP code is used to deduce energy, angular momentum, and density transport. The physics-based predictive models GLF23 and MMM95 are used to simulate temperature and toroidal velocity profiles assuming turbulence driven by ITG/TEM. The GYRO gyrokinetic code is used for nonlinear turbulence simulations of the energy, angular momentum, and species transport during quasi-steady state phases. Modeling and simulation results are compared to experimental measurements with limited agreement, indicating that further work is still required. Effects of varying the negative ion neutral beam injection into simulated ITER Hybrid plasmas indicates that below-axis aiming can maintain the q profile above unity.

1. Introduction Hybrid discharges are so called as they combine advantages of the H-mode and Steady State regimes to address the ITER long pulse, high fluence mission. Common features of Hybrid plasmas are central safety factors near or above unity, with sustained stationary high β_n, high confinement, and reduced inductive current relative to standard H-mode plasmas of equivalent fusion performance. Some of the issues that need to be addressed for confidence in the ability to create Hybrid plasmas in ITER are: 1) Can high values for the product $n_d n_t$ be maintained where T_i is high? 2) Can high confinement (e.g., β_n) be achieved and sustained? 3) Are large external torques required (e.g., to create sufficient flow shearing rates)? 4) Can an appropriate q profile be achieved and maintained? 5) Is a high edge pedestal required? Credible predictions of ITER hybrid performance depend on the successful validation of simulation codes on existing experiments. Also since large extrapolations from conditions in present plasmas to burning

plasmas are needed, it is important to base the predictions on rigorous calculations such as those using gyrokinetic codes as much as possible.

Previous studies [1,2] of hybrid plasmas in the ITPA database tested predictions of various models such as GLF23 [3] and MMM95 [4]. In general, the model profile predictions in this previous work did not agree well with experiment. Also linear simulations found regions of stability (linear growth rates below zero) extending out to unusually large r_{min}/a ($\simeq$ 0.5-0.7). This later result is paradoxical since power-balance-derived energy flows are relatively large (at least several times neoclassical) in this region. This paper extends the work of [1,2] to address the modeling/experiment discrepancies found there by: 1) Using new submissions to the ITPA profile database; 2) New predictive modeling of temperature profiles using the GLF23 and MMM95; 3) Nonlinear gyrokinetic turbulence simulations of energy, momentum, and particle flows using GYRO [5] over extended radial regions with kinetic electrons, two kinetic ion species, and $E \times B$ flow shear; 4) Since the maximum flow shearing rate in ITER (excluding the pedestal region) is expected to be lower than typical values in JET and DIII-D by factors of about 10, we scaled down the measured flow shear by this amount to test the reliability of direct extrapolations of performance to ITER; and 5) Studies of effects of NNBI aiming in ITER Hybrid plasmas. However, as shown below, even with these updates and extensions, substantial disagreements between modeling and experiment remain, and potential reasons for this are presented.

2. Updates to the profile database and Phenomenology A number of recent JET Hybrid plasmas, including some with tritium gas puffs have been analyzed and are ready for submission to the ITPA profile database. Several ASDEX-Upgrade Hybrid plasmas have been analyzed by TRANSP [6], and are ready for submission. The phenomenology of Hybrid plasmas remains not well understood, and there may in fact be a variety of Hybrid regimes. Diverse MHD phenomena are observed: benign 3/2 NTM, fishbones, minor sawteeth, and even, on occasion, no MHD. A recent study [7] of transport in JET H-mode and Hybrid plasmas indicates that differences in their transport are not obvious, but subtle differences were noted, such as n_e and n_{imp} being more peaked in Hybrid plasmas and n_d being less peaked. One speculation is that peaking is related to the absence of sawteeth mixing in Hybrid plasmas. Also the ratio $\tau_{momentum}/\tau_E$ appears lower for Hybrid plasmas, and decreases as the ratio of the average NBI torque per particle increases. Hybrid plasmas tend to have high P_{NBI} and thus high torque. A curious feature of some of the DIII-D Hybrid plasmas is the indication that anomalous fast ion losses often appear needed in the TRANSP analysis to reconcile the simulated and measured total energies and neutron emission rates. This may be related to the presence of core Alfvén modes [8].

3. Predictive Models Hybrid plasmas appear to pose a more challenging test of transport models than standard H-mode plasmas because they generally have higher confinement and β_n, and a wider variety of magnetic shear, and expected stronger roles of $E \times B$ and alpha stabilization. High confinement indicates that they are in domains of reduced turbulence, increased stabilization, or a combination of the two. The simulations reported here explore some of the sensitivities.

Various transport codes use models to predict plasma parameters such as temperatures and toroidal rotation profiles. These are being used to simulate measured profiles and to predict performance in ITER. In principle they need profiles of the flows of energy, torque, and densities which can either be calculated internally or input from the database, relying on the accuracy of the profiles in the database. For self-contained simulations of experiments and predictions for ITER, the transport codes will need to calculate these. Important issues for these codes are: 1) Accuracy of the calculations of the heating, current drive, and torques; 2) Accuracy of numerical solutions to the typically stiff equations in the predictive models; 3) Effects of the $E \times B$ shearing rate and the fact that often large neutral beam-induced toroidal velocity is the dominant

term for the $E \times B$ shear stabilization; 4) Effects of alpha stabilization; 5) Effects of neutral beam ions including their pressure; 6) Threshold for stability; 7) Transport mechanisms in turbulence stable regions; and 8) Potentially significant physics not included, such as finite ρ_* effects and turbulence spreading.

We report on results from predictive modeling using four representative transport codes: 1) ASTRA [9] with GLF23 and MMM95, 2) CRONOS [10] with GLF23, 3) TSC [11] with GLF23, and 4) XPTOR [12] with GLF23. The first three codes have varying ability to internally compute fluxes from heating and current drive models. All four can read data from the ITPA profile database. ASTRA and TSC can also read data from the TRANSP runs used to generate the data for the ITPA profile database. All four can compute the time evolutions of the temperature profiles assuming boundary conditions near the top of the pedestal, typically taken near $r_{min}/a = 0.8\text{-}0.9$.

Three of the most studied Hybrid plasmas were chosen for comparisons of predictions. Table I lists some of the plasma parameters and gives a projected ITER Hybrid scenario (also in the ITPA database) generated with predictive TRANSP (pTRANSP) for comparison. The analysis times listed are during high performance, quasi-steady state phases. The Greenwald fraction $f_{GW} \equiv \overline{n}_e/(I_p/(\pi r_{min}^2))$ and H_{89} are given. The JET 58323, from a JET-ASDEX Upgrade identity experiment [13] has a figure of merit $H_{89}\beta_n/q_{95}^2 = 0.4$ lasting 4s. It also had a large fast beam ion density with $n_{beam} = 0.5n_d$ in the core. This and the DIII-D Hybrid had T_i/T_e considerably higher than unity, a disadvantage for extrapolating to ITER.

Table I: Parameters of plasmas considered at quasi-steady state times

Tokamak	shot	time	B_0	I_p	κ	δ	q_{95}	P_{nbi}	β_n	f_{GW}	H_{89}
	units	[s]	[T]	[MA]	elong	triang		[MW]			
JET	58323	12.1	1.8	1.4	1.6	0.3	4.0	15.4	2.8	0.50	2.1
JET	60931	10.85	1.7	1.4	1.8	0.5	4.8	16.8	2.4	0.60	1.7
DIII-D	104276	5.0	1.7	1.22	1.8	0.5	5.0	6.0	2.3	0.38	3.0
pTRANSP ITER	20020100	400.0	5.3	12	1.8	0.5	4.5	33.0	3.1	0.93	

ASTRA computes the time evolutions typically starting about 2 sec before the time of interest. The heating, torque, and q profiles were read from TRANSP runs. Figure 1 compares temperature predictions for JET 58323 at a time slice with measurements (mapped by TRANSP). $E \times B$ shear and alpha-stabilization were used. Results using either MMM95 or GLF23 are shown. MMM95 predicts central T_i and T_e lower than their measured values by as much as 35%. GLF23 was used with different assumptions to test their validity: either including the TRANSP-computed beam density or ignoring it, and either using the measured v_{tor} or predicting it. The v_{tor} profile is used for computing the $E \times B$ flow shearing rate. GLF23 computes the thermal ion density from the input n_e, Z_{eff}, and n_{beam} if provided. The predictions ignoring n_{beam} and simulating v_{tor} are close to the measured values. ASTRA-GLF23 was also used to predict v_{tor} with and without inputting n_{beam} to GLF23. The result ignoring n_{beam} is about three times higher than the measurement, and the result including n_{beam} is about twice. Thus including n_{beam} is bad for predicting T_i, but good for v_{tor}.

The CRONOS-GLF23 simulations input the plasma profiles from the ITPA database and compute the evolutions of the heating, current drive, and typically the q profiles. The v_{tor} profiles are read from the database. Alpha stabilization is included with alpha typically calculated including the fast ion pressure. Figure 2 compares simulations of JET 58323 with internally-computed or input q, and with or without including fast ion effects (n_{beam} and the fast pressure for the equilibrium calculation). In the usual mode, CRONOS evolves q self-consistently. For comparison, the q evolution was fixed when the profile approximated the one in the
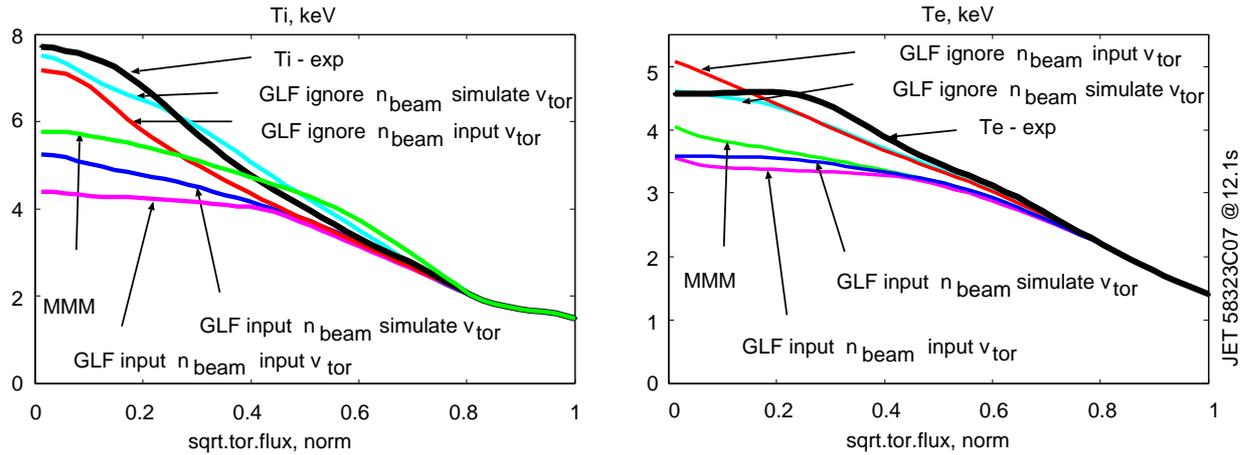
FIG. 1: ASTRA temperature predictions for JET 58323 using GLF23 and MMM95.

ITPA database profile (derived using EFIT). The predictions without using the fast ion density and pressure are closest to the measurements. Note the different direction of the effects of n_{beam} in the ASTRA and CRONOS results: increasing T_i in ASTRA and decreasing in CRONOS. This could be a consequence of changes in the stability threshold with changed n_d.
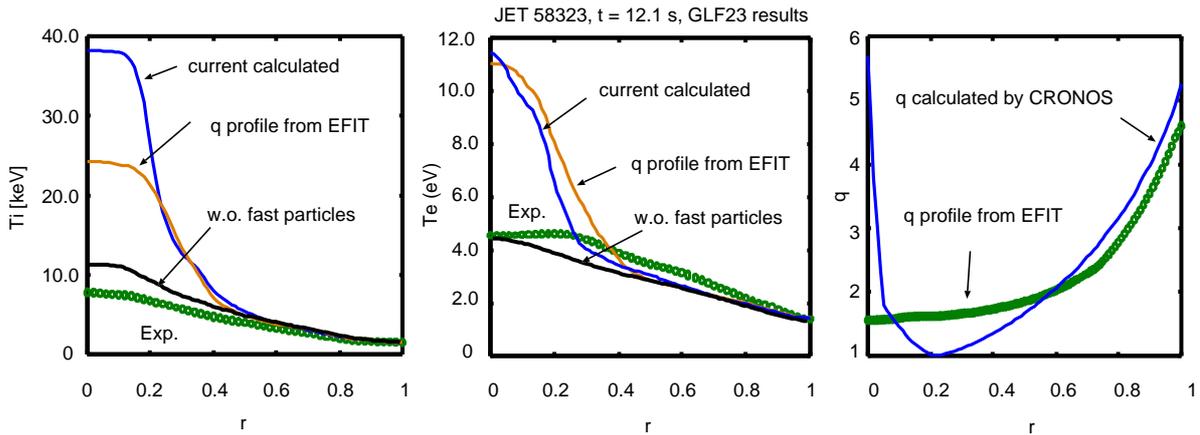
FIG. 2: CRONOS-GLF23 simulations of T_i, T_e and q for JET 58323

Profiles of the computed linear ITG growth rate for JET 58323 from the GKS code are shown in Fig 3a with and without flow shearing suppression. The plasma is predicted to be stable for r_{min}/a less that 0.35. Predictions of the temperatures from XPTOR are shown in Fig. 3b. The predicted T_i including $E \times B$ shear agrees well, but the predicted core T_e is low both with and without $E \times B$ shear.

JET 60931 was also modeled with ASTRA, CRONOS, and XPTOR. This shot has T_i close to T_e and a lower n_{beam} than 58323. Greater success and less variation of results with different modeling choices was achieved.

Figures 4-6 compare simulations for DIII-D 104276. Figure 4 shows ASTRA-GLF23 results from two TRANSP runs, one (in the database) with anomalous fast ion diffusion assumed to be $0.3 m^2/s$, and the other with none. The anomalous diffusion makes a 35% reduction of n_{beam} in the core, but did not have a large impact in the predicted temperatures. The modeling choices that worked best in Fig. 1 gave poor results in this case.
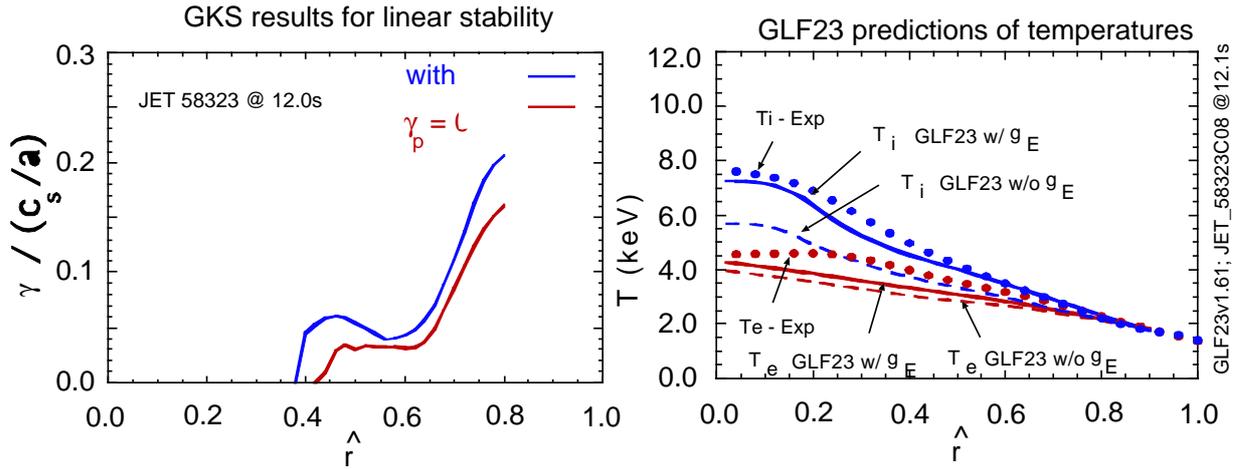
FIG. 3: GKS linear stability for JET 58323; b) XPTOR-GLF23 predictions.

For the TSC-GLF23 simulations shown in Fig. 6 the heating power profiles were taken from TRANSP and q was calculated. The n_{beam} was not input to GLF23, and the alpha stabilization was not turned on. Simulations with and without rotation for flow shearing suppression are shown. Note that the results for T_i with rotation are best, and the results for T_e without rotation are best. The full time-evolution was modeled, and the evolutions of the central temperatures are also shown. The data shows an ITB forms in T_i during the L-mode phase, but disappears when the H-mode phase forms. The GLF23 prediction failed to model the ITB.
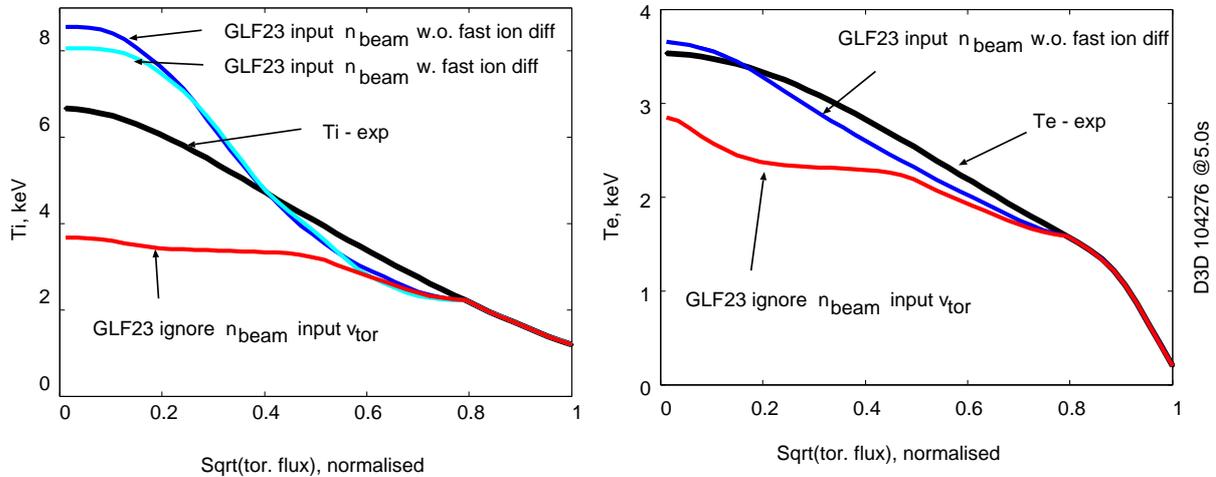
FIG. 4: ASTRA-GLF23 temperature predictions for DIII-D 104276 from two TRANSP runs, one with anomalous fast ion diffusion and one with none

As can be seen from these comparisons, in general the transport models do not replicate the experimental profiles very well. Reasons for this discrepancy could include: 1) Fundamental limitations of simplified transport; 2) Model implementation in code; 3) Numerical accuracy issues; 4) Other physics not captured in transport models, e.g.. MHD/coherent mode activity, turbulence spreading, realistic flux surface geometry, and impurities. Some of these can be addressed by the nonlinear calculations presented in next section.
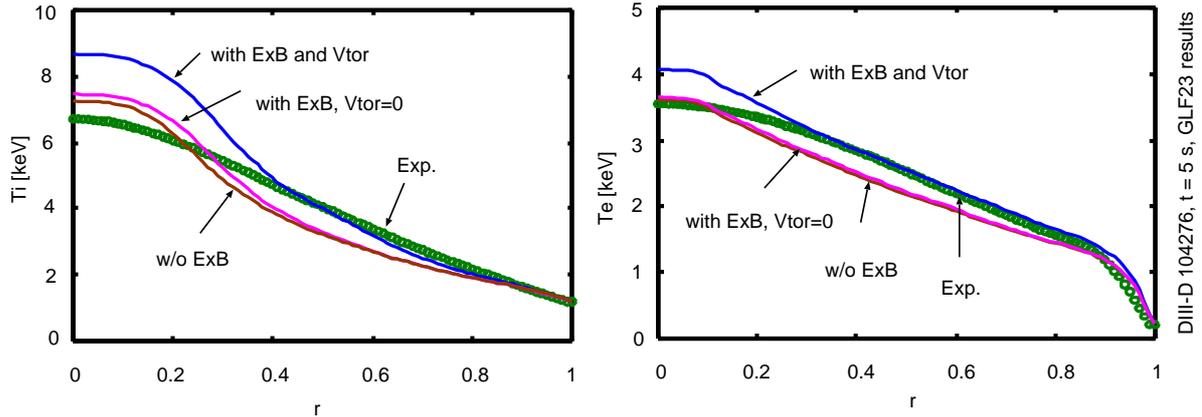
FIG. 5: CRONOS-GLF23 temperature predictions for DIII-D 104276
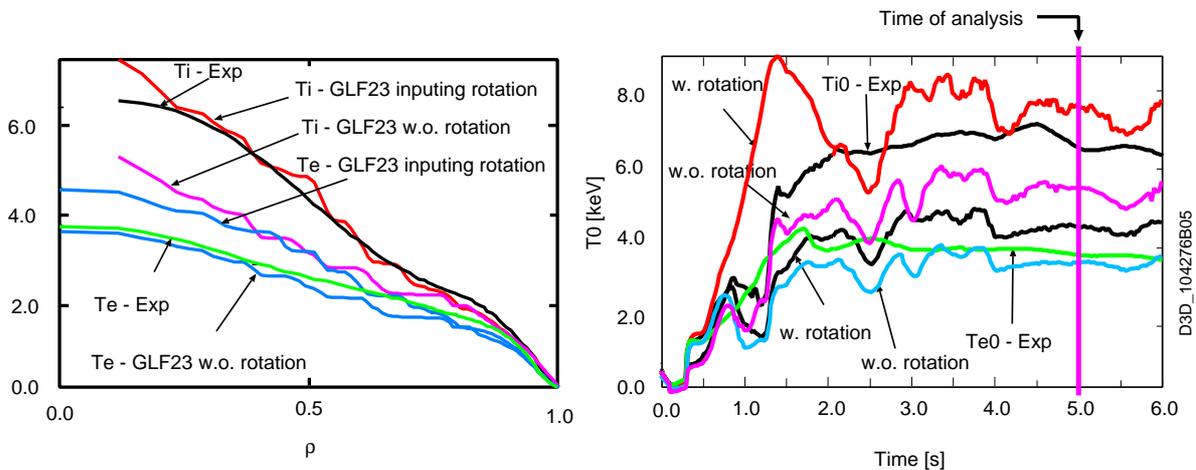
FIG. 6: TSC-GLF23 temperature predictions for DIII-D 104276

4. Nonlinear gyrokinetic simulations Gyrokinetic codes contain physics not in the predictive models, and offer the possibility to calculate the turbulence-driven transport that often dominates the radial flow of energy, angular momentum, and density in tokamak plasmas. We present the first results using GYRO for Hybrid plasmas. In GYRO there are no relevant physically-measurable free parameters left unspecified. Some of these parameters can be varied for computational expediency, such as the electron to ion mass ratios. Some of the physical processes can be turned on or off such as the Kelvin-Helmholtz drive, external $E \times B$ flow shearing rate, collisions, and electromagnetic (EM) corrections to the electrostatic (ES) turbulence in order to study their effects. There are many parameters controlling the numerics, such as box size, radial grid, energy grids, number of toroidal modes, time stepping, etc. The physics has to be independent of these, so these need to be varied to check the numerical accuracy.

The usual way to run GYRO is to specify measured plasma profiles and use their drive terms to calculate the implied turbulence-driven evolution of the distribution functions. The distribution functions of each of the "kinetic" species are computed, and moments of them give the transport of energy, angular momentum, and the densities of the kinetic species. Long-wave adaptive sources/sinks in GYRO keep the equilibrium profile gradients fixed. The distribution functions are renormalized at each time step by summing over pitch angle, projecting on the longest radial wavelengths in the box, and subtracting this result out. This has the effects of removing temporal drifts of the plasma profiles away from their measured mean-values.

We performed the GYRO simulations over an extended radial domain around the plasma mid-radius, treating three kinetic species: bulk ions, lumped impurities, and electrons. The input profiles are deduced from TRANSP analysis runs at relatively steady state times. The outputs include profiles of energy, angular momentum, and density transport.

Table II: Plasma parameters near the half-radius

Tokamak	shot	ρ_*	R/L_{Ti}	R/L_{Te}	R/L_{nmain}	R/L_{nimp}	R/L_{ne}
JET	58323	0.00392	6.29	3.07	1.91	-2.75	1.15
JET	60931	0.00336	7.33	6.67	1.47	-2.98	1.07
DIII-D	104276	0.00441	5.29	4.13	3.59	0.021	2.76
pTRANSP ITER	2002000	0.00112	4.33	3.83	1.73	-4.28	1.21

An important input for the simulations is the beam-driven flow shearing rate. This is calculated from E_r given from force balance for carbon using the measured v_{tor}, p_{carbon}, and v_{pol} from NCLASS [14]. The neutral beam-driven torque density in ITER will be about 10% that in current Hybrid plasmas, so we also did GYRO runs with the external flow shearing rate scaled down by a factor of 10 to test the scaling to plasmas with reduced flow such as that expected in ITER. Nonlinear GYRO runs in both the ES approximation and with EM corrections have been done for the three Hybrid shots discussed in the previous section. Table II shows normalized scale lengths of these plasmas.

The upper panels in Fig. 7 shows the GYRO inputs for the JET Hybrid 58323. The simulation domain lies between $r_{min}/a = 0.35$ and 0.85, with a width of about 128 ion gyro-radii ρ_s. This is sufficiently wide to allow growth of turbulent eddies. The temperature and density profiles are measured, but the q profile was not for either of the JET Hybrids. The profile shown is from EFIT analysis, and there is considerable uncertainty about the central values. The main kinetic ion species is thermal deuterium and the second kinetic species is a combination of the measured carbon density and the calculated beam ion density, with A_{eff} and Z_{eff} chosen to conserve local charge neutrality.

The lower panels in Fig. 7 compare the simulations and measurements for the total (diffusive and convected) ion energy flow and the diffusive angular momentum flow. The profiles shown in black labeled TRANSP are from analysis using local conservation of ion thermal energy and angular momentum. The red curves give the simulations assuming the EFIT profile and the nominal profile of the E_r flow shearing. The inaccurately-known q profile was scaled up or down by 10 or 20% to explore consequences of the uncertainty. The orange, green, and blue curves give results with the EFIT q profile scaled down by 20%. The blue curves give the GYRO simulation (in the ES approximation) assuming flow shear given by measurements ($1.0E_r'$). The simulated ion energy flow is close to the measured value in the middle of the radial domain. The simulated transport tends to decrease as the q profile is decreased towards unity, suggesting that the optimal q is just above the sawtoothing limit. The simulated angular momentum flow is about 2.5 times the measured value. The Kelvin-Helmholtz instability is a significant contributor to the simulated flow, and simulations with it turned off give angular momentum flows negative in some regions indicating a pinch, not seen in the data.

The green simulations in Fig. 7 used the assumption that E_r' is scaled up by 1.1 to explore the sensitivity of the simulation. This is within experimental uncertainties, particularly given the fact that the assumption that the poloidal flow is purely neoclassical may not reflect reality. This simulated ion energy and angular momentum flows are close to the measurements in the middle of the box, but low at larger radii. This
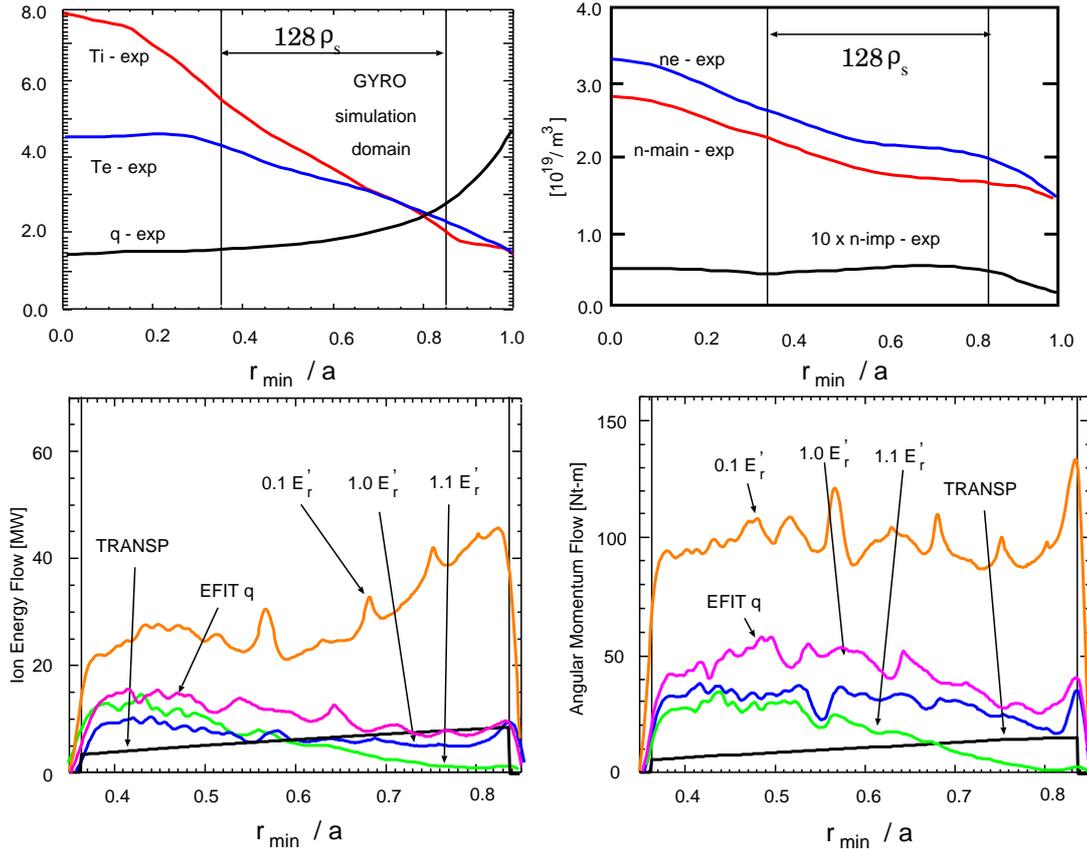
FIG. 7: GYRO input profiles for JET 58323

variation with E_r' shows an example of the high sensitivity of the simulations to drive or damping with plasma conditions very close to marginal.

The orange simulations in Fig. 7 assume that the external flow shearing rate is scaled down by a factor of 10 to test the extrapolation to plasmas with reduced flow such as that expected in ITER. This causes the turbulent ion energy flow to increase significantly. Peaks in the simulated profiles occur around low order rational surfaces. The simulated effective electron density diffusivity D_e, defined from $\Gamma_e \equiv -D_e A_{surface} \nabla(n_e)$ is positive within $r_{min}/a = 0.66$, and negative further out indicating a plasma pinch, i.e. flow up a density gradient The simulation of the analogous main ion effective diffusivity has the same qualitative features, but the impurity ion effective diffusivity is positive across the simulation domain, and the impurity density is hollow ($\nabla(n_{imp}$ positive), so the flux is predicted to go outward.

Similar simulations of the other two Hybrid plasmas with the ES approximation were not as close to measurements as those shown in Fig. 7. For JET 60931 the peak of the ion energy flow was too high by a factor of 2.5. Turning on the EM corrections in GYRO gave a significant improvement, with the simulation being high only 70% near the mid-radius, and close to measured near the edges of the simulation region ($r_{min}/a \simeq 0.45$ and 0.75).

The simulations for the DIII-D Hybrid over the range r_{min}/a 0.12-0.83 indicate no turbulence within 0.3, and a peak ion energy flow near $r_{min}/a = 0.7$ too high by a factor of 5. Turning on EM corrections (with the assumption that the square-root of the main ion to electron mass is 20 instead of close to 60 for computational expediency) gave significant, but not sufficient reductions of the flow. The nonlinear GYRO results for another DIII-D Hybrid (118446) indicate that significant amount of transport occurs at large

values of $k_\theta \rho_s$, suggesting TEM and/or ETG dominance. The turbulence is low, contrary to the power balance results, but this stability depends sensitively on T_i which is sufficiently greater than T_e for T_i/T_e drive, as well as on $|\nabla(T_i)|$ and the $E \times B$ shearing rate. Thus even the full gyrokinetic simulations are not replicating experiments very well, and further work is needed.

We also did a set of ES nonlinear runs to estimate the relative importance of drive and damping terms on the transport, and to explore whether variations of profiles within the experimental errors could account for the discrepancies in the simulated transport. For this we compute the changes in the energy, species, and angular momentum transport coefficients as we varied the drive/damping terms from their measured values by $\pm 20\%$. Besides the usual diagonal terms, many of the off-diagonal terms have significant and complicated contributions to the transport. Results for the JET 60931 averaged over the region r/a between 0.4 and 0.8 indicates that χ_e is driven mainly by $\nabla(T_{bulk})$ and $\nabla(n_{bulk})$; the electron species flow Γ_e is driven inward by $\nabla(T_{bulk})$, $\nabla(T_e)$, $\nabla(n_{bulk})$ and outward by $\nabla(n_e)$ with a net inward pinch; and Γ_{imp} is driven outward by $\nabla(T_e)$, $\nabla(n_{bulk})$, and $\nabla(n_{imp})$, and inward by $\nabla(n_e)$. The electron and impurity flows have the additional complication that the contributions of modes with relatively low and higher $k_\theta \rho_s$ are in opposite directions. For two of the JET hybrids, the simulated energy flows are close to marginal, but higher than the power-balance-derived flows. This result is similar to the previous results for JET standard H-mode plasmas [15].

5. Implications for ITER Predictive models such as GLF23 are being used to simulate ITER plasmas and several examples have been submitted to the ITPA profile database for further study and use. Parameters for one of the cases were given in Tables I-II. Effects of NNBI aiming, as planned for ITER, have been studied using pTRANSP. Significant effects on the beam-driven current near the plasma axis, and thus on the central q-profile are found below-axis aiming into hybrid plasmas is expected to sustain q above unity for long ($> 800s$) durations. Examples of beam trajectories and the central q values are shown in Figure 8. The indication that NBCD can maintain q above unity might obviate the need for benign NTM's to effect the q profile, as is often the case with present hybrid plasmas, or for alternatives such as ECCD or LHCD. Having to rely on benign NTM's could have other restrictive consequences such as requiring operation with very high values of β_n and T_{ped}.
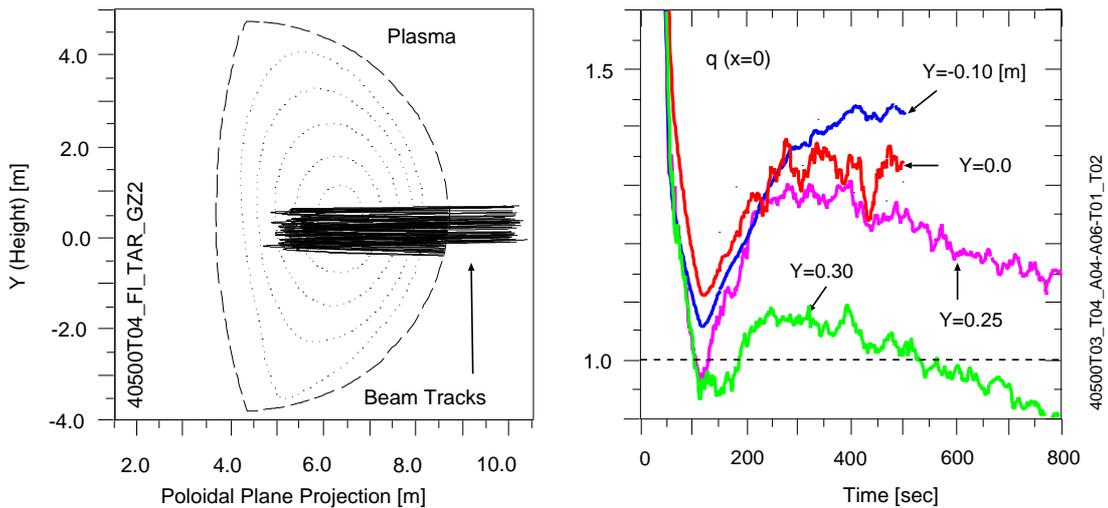
FIG. 8: pTRANSP simulation of NNBI steering effects into a ITER Hybrid plasma predicted by TSC-GLF23.

6. Discussion New Hybrid plasmas are being submitted to the profile database and better understanding of their transport is accumulating. Predictive models such as GLF23 are being used to simulate the temperatures and toroidal velocities. A special challenge of Hybrid plasmas to theory-based transport models is in describing the eigenmodes at low-q and low magnetic shear. GLF23 was developed using a reference case with q=2.0 and $\hat{s}$=1.0. There are indications that the ITG mode structure differs from the usual structure simulated in H-mode and L-mode plasmas by having non-zero values extending over a much larger region in ballooning angle. This extended structure creates challenges for the GLF23 modeling. At low-q the modes are typically very non-Gaussian and extended in ballooning angle.

Different results and different degrees of success in predicting experimental measurements are achieved with differing assumptions about the treatment of the beam density, toroidal velocity, and alpha stabilization. GLF23 results can be sensitive to various modeling aspects (e.g. how the fast ions are handled) and the same methodology needs to be employed for useful code comparisons. This indicates a need for a new initiative of predictive benchmarking with controlled sets of profiles and assumptions about input settings. Implementation of the models in different simulation codes also show that as yet unresolved differences in implementation of the models (input to the models and treatment of the non-linear fluxes and transport coefficients) also need to be resolved.

Extensive nonlinear modeling of a few of the Hybrid plasmas from JET and DIII-D have been done with the GYRO code. The simulated ion energy transport shown above is within 80% of the mid-radius measured value. Results for other Hybrids with the ES approximation are high by up to a factor of 5. Including electromagnetic effects give significant improvements, but they have not been studied extensively since they are much more CPU intensive than the electrostatic effects typically calculated. They are expected to reduce ion energy transport closest to the core where β is largest. Calculations to test this hypothesis using GYRO are ongoing. The simulated angular momentum and density transport shows some of the qualitative features seen in measurements, but more work is needed. Due to the strong sensitivities of the simulations to input assumptions, accurate measurements would help test the theory. Examples are accurate q and E_r profiles and fluctuations.

Noteworthy results of the simulations are: 1) Reduction of transport as q is lowered toward the sawtoothing limit; 2) Significant increases in transport as the flow shearing rates are reduced to values expected for ITER; and 3) Significant contributions of off-diagonal drive to the turbulent transport.

[1] J.E.Kinsey, F.Imbeaux, G.M.Staebler, R.Budny, C.Bourdelle, *et al.,* Nucl. Fusion **45** (2005) 450.
[2] F.Imbeaux, J.F.Artaud, J.Kinsey, T.J.J. Tala, *et al.,* Plasma Phys. Cont. Fusion **47** (2005) B179.
[3] R.E.Waltz, G.M Staebler, W.Dorland, G.W.Hammett, *et al.,* Phys. Plasmas **4** (1997) 2482.
[4] G. Bateman, A.H. Kritz, J.E. Kinsey, A.J. Redd, and J. Weiland, Phys. Plasmas, **5** (1998) 1793.
[5] J.Candy and R.E.Waltz, Phys. Rev. Lett. **91**, 045001 (2003).
[6] R.V.Budny, D.R.Ernst, T.S.Hahm, D.C.McCune, *et al.,* Nuclear Fusion, **7** (2000) 5038.
[7] I.Voitsekhovitch, R.Budny, E.Joffrin, *et al.,* EPS, Rome, 2006, paper P1.078
[8] R.Nazikian, H.L.Berk, R.Budny, K.H.Burrell, E.J.Doyle, *et al.*, Phys. Rev. Lett. **96**, 105006 (2006)
[9] G.V.Pereverzev, P. N. Yushmanov, Report IPP 5/98, 2002
[10] V. Basiuk, J.F. Artaud, F. Imbeaux, X. Litaudon *et al.*, Nucl. Fusion **43** (2003) 822-830
[11] S.C. Jardin, N. Pomphrey, and J. Delucia, J. Comput. Phys., **46** (1996) 481.
[12] J.Kinsey, G.M Staebler, R.E.Waltz Phys. Plasmas **9** (2002) 1676.
[13] E.Joffrin, A.C.C.Sips, A. Becoulet, L. Bertalot, R. Budny, *et al.,* Nucl. Fusion **45** (2005) 626.
[14] W. Houlberg, K. Shang, S. Hirshman, and M. Zarnstorff, Phys. Plasmas **4** (1997) 3230.
[15] R.V.Budny, J.Candy, and R.E.Waltz, EPS, St. Petersburg, July, 2003.